Measurement 94 (2016) 883–892

Contents lists available at ScienceDirect

Measurement

journal homepage: www.elsevier.com/locate/measurement

Accuracy and noise analyses of 3D vibration measurements using laser Doppler vibrometer

Hossam Khalil, Dongkyu Kim, Joonsik Nam, Kyihwan Park *

School of Mechanical Engineering, Gwangju Institute of Science and Technology, 123 Cheomdangwagi-ro, Buk-gu, Gwangju 61005, South Korea

ARTICLE INFO

Article history:
Received 10 April 2016
Received in revised form 29 July 2016
Accepted 3 September 2016
Available online 6 September 2016

Keywords:
Accuracy of 3D vibration measurement
2D vibration measurement
Laser Doppler vibrometer (LDV)
Laser scanning vibrometer (LSV)
Angle analysis

ABSTRACT

The in-plane and out-of-plane vibration components are used for 3D vibration measurements. The latter can be calculated by using three laser scanning vibrometers (LSVs) or by moving a single LSV to three different locations. These vibration components are calculated from the vibration signals measured at each of the three locations and the angles between the local coordinates and the LSV locations. The accuracy of the in-plane and out-of-plane vibration components can be degraded depending on the measurement angle. In addition to accuracy, the noise contained in the LSV can be amplified depending on the measurement angle. Hence, it is necessary to implement an analysis methodology for the angles, which is conducted for 2D vibration measurements first before extended to 3D. Finally, experiments are performed for both 2D and 3D at small and appropriate angles, and the elicited results are compared to those elicited using a 3D accelerometer.

1. Introduction

Accelerometers have been traditionally used for vibration measurements in conventional modal testing. These contact-type sensors have several disadvantages, including loading effect that change the natural frequencies of light and flexible structures. These sensors cannot measure vibration signal unless they are attached to the object. Ultimately, there is a high sensitivity to electromagnetic interference which makes it difficult to measure the vibration of electronic components. Furthermore, in order to obtain the mode shape of the entire surface, it is necessary to use multiple sensors [1].

These problems can be solved using a noncontact laser Doppler vibrometry (LDV) [2,3]. An LDV measures the velocity signal of an object using the Doppler frequency shift due to the interference between the incident and scattered light reflected from the surface of a vibrating object. LDVs are considered to be a technology that could rapidly and correctly measure the vibration of a desired position. To estimate the mode shapes considering the measurement of the entire surface, the vibration of multiple points can be easily measured using a pair of electric motors combined with the use of an LDV, an instrument which is known as a laser scanning vibrometer (LSV).

For measuring true vibration that occurs in an object, three sets of LSV are needed. This is because the vibration of the object can occur along three distinct directions [4]. 3D vibration measurements using LSVs, called a 3D scanning laser Doppler vibrometer (3D-SLDV) are increasingly needed for various industrial applications because of their accurate and high-speed measurements. 3D-SLDV is used to measure true vibration in many applications. For example, in [5] it was used to measure the vibration of power tool, in [6] bridge vibration measurements, in [7] the measurement of 2D dynamic stress distributions, and in [8] structural health monitoring using ultrasonic surface waves.

A new algorithm for 3D vibration measurements is introduced in [9] using just one LSV set rather than three sets of LSVs, which has a notable disadvantage due to the high cost. This method has the same effect in regard to the use of the three sets of LSVs since a vibration analysis in the frequency domain is independent of the time at which the vibration becomes uniform. For 3D vibration measurements of an object, it is required to measure the vibration of points on the object at three different locations. The proposed method in [9] is a good approach for obtaining the 3D vibration components.

From the measured vibration signals at three arbitrary positions, and the angles between the local coordinates and the LSV locations, the vibration components of the in-plane and out-of-plane directions are calculated. However, the accuracy of vibration in the in-plane and out-of-plane components can be degraded depending on the measurement angles. In addition to the accuracy problem, the noise contained in the LSV signal can be amplified depending on the measurement angles. Hence, it is necessary to introduce an analysis methodology for the angles so that the accuracy of the vibration measurement can be increased, and the noise

* Corresponding author.
E-mail address: khpark@gist.ac.kr (K. Park).

http://dx.doi.org/10.1016/j.measurement.2016.09.003
0263-2241/

minimized. The accuracy and noise levels are the most important issues for 3D vibration measurement.

For the sake of simplicity, the analysis of the angles is implemented for 2D vibration measurements first before 3D vibration measurements are addressed. This is experimentally investigated for small and appropriate angles for both 2D and 3D vibration measurements. All of these results are compared to those measured from 3D accelerometers.

In Section 2, the principle of the algorithm for the 3D vibration measurement is introduced. The sensitivity of the angles for accurate velocity measurements and noise reduction is discussed in Section 3. In Section 4, experiments for both 2D and 3D vibration measurements are introduced.

2. Principle of 3D vibration measurement algorithm

For measuring true vibration occurred in an object, the LSV moves to three different locations, namely, $(x_1, y_1, z_1), (x_2, y_2, z_2)$, and (x_3, y_3, z_3), as shown in Fig. 1. The measuring point on the object's surface is defined using the local coordinates (x_o, y_o, z_o) where the direction of the x_o-axis is parallel to the x_2z_2 plane, whereas the direction of the y_o-axis direction is perpendicular to the x_oz_o plane. The direction of the z_o-axis is thus perpendicular to the surface of the object containing the measuring point. Suppose that the vibrations measured at three arbitrary locations are V_1, V_2, and V_3. The angles between the local coordinates (x_o, y_o, z_o) and V_1, V_2, and V_3, are defined as α_k, β_k, and γ_k, where $k = 1, 2$, and 3. If V_x, V_y, and V_z, are the vibration components of the measuring point in the directions of local coordinates (x_o, y_o, z_o), these are then calculated using V_1, V_2, and V_3, and the angles $(\alpha_k, \beta_k, \gamma_k)$ as

$$\begin{pmatrix} V_x \\ V_y \\ V_z \end{pmatrix} = \begin{pmatrix} cos\alpha_1 & cos\beta_1 & cos\gamma_1 \\ cos\alpha_2 & cos\beta_2 & cos\gamma_2 \\ cos\alpha_3 & cos\beta_3 & cos\gamma_3 \end{pmatrix}^{-1} \begin{pmatrix} V_1 \\ V_2 \\ V_3 \end{pmatrix} \quad (1)$$

Since V_1, V_2, and V_3, can be transformed into the frequency domain as FRF_1, FRF_2, and FRF_3, then FRF_x, FRF_y, and FRF_z that are transformed into the frequency domain from V_x, V_y, and V_z can also be calculated using FRF_1, FRF_2, and FRF_3, and the angles $(\alpha_k, \beta_k, \gamma_k)$ as

$$\begin{pmatrix} FRF_x \\ FRF_y \\ FRF_z \end{pmatrix} = \begin{pmatrix} cos\alpha_1 & cos\beta_1 & cos\gamma_1 \\ cos\alpha_2 & cos\beta_2 & cos\gamma_2 \\ cos\alpha_3 & cos\beta_3 & cos\gamma_3 \end{pmatrix}^{-1} \begin{pmatrix} FRF_1 \\ FRF_2 \\ FRF_3 \end{pmatrix} \quad (2)$$

For simplicity, the angle analysis is implemented for 2D vibration measurements first, before 3D vibration measurements are addressed.

Herein, the 2D vibration measurement algorithm is discussed. Fig. 2(a) and (b) shows the geometric relation of the 2D vibration measurement system at 3D and 2D views, respectively. Herein, the vibration signals measured at the two arbitrary locations are V_1 and V_2. The respective angles between the x_o-axis and (V_1, V_2) are α_1 and α_2. Correspondingly, the respective angles between the z_o-axis and (V_1, V_2) are γ_1 and γ_2. V_x and V_z are then simply obtained using the general relation of Eq. (1) as

$$\begin{pmatrix} V_x \\ V_z \end{pmatrix} = \begin{pmatrix} cos\alpha_1 & cos\gamma_1 \\ cos\alpha_2 & cos\gamma_2 \end{pmatrix}^{-1} \begin{pmatrix} V_1 \\ V_2 \end{pmatrix} \quad (3)$$

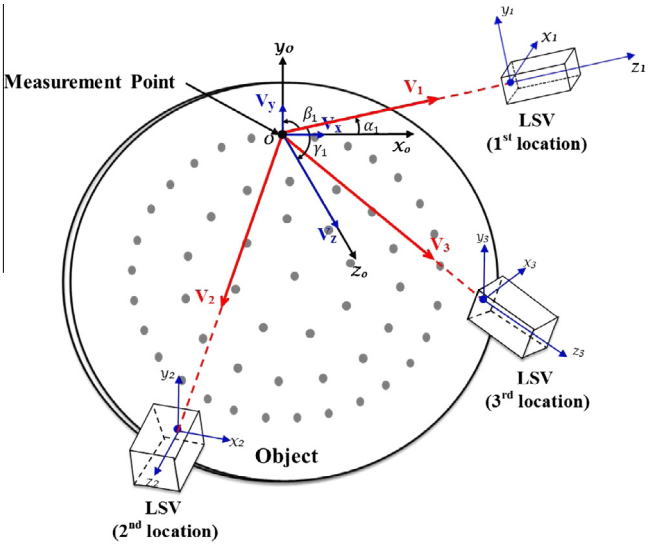

Fig. 1. Configuration of the system for 3D vibration measurements.

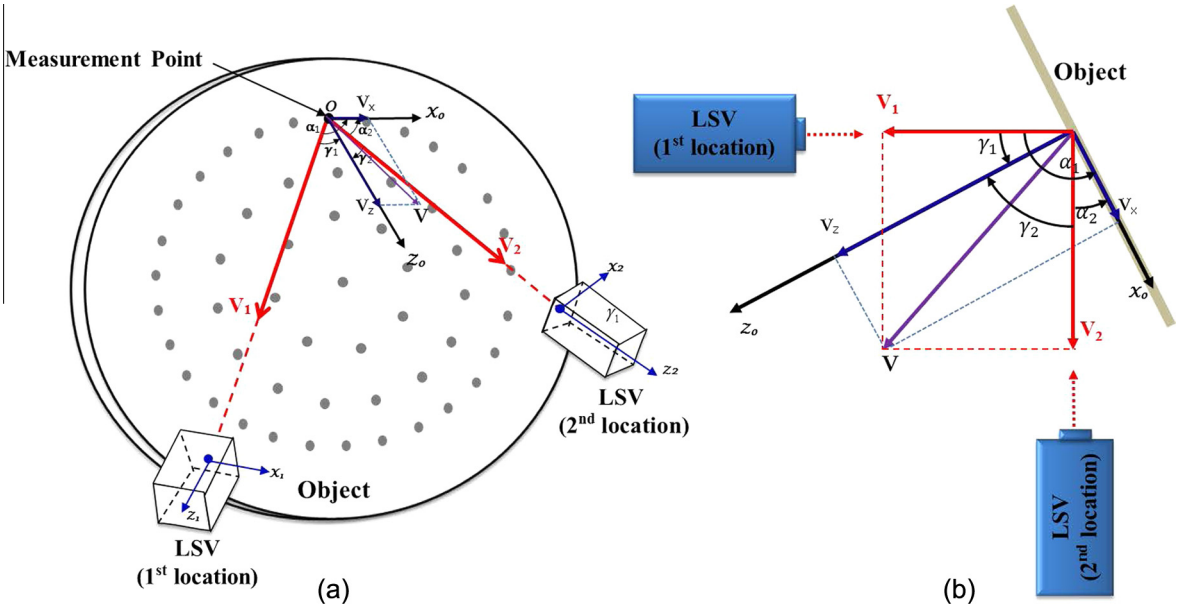

Fig. 2. Geometric relations of the 2D vibration measurement system in (a) 3D view, and (b) 2D view.

Eq. (3) can be rewritten in accordance to Eqs. (4) and (5).

$$V_x = \frac{V_2 cos\gamma_1 - V_1 cos\gamma_2}{sin\gamma_1 cos\gamma_2 + cos\gamma_1 sin\gamma_2} \tag{4}$$

$$V_z = \frac{V_2 sin\gamma_1 + V_1 sin\gamma_2}{sin\gamma_1 cos\gamma_2 + cos\gamma_1 sin\gamma_2} \tag{5}$$

Then, FRF_x and FRF_z that are transformed into the frequency domain from V_x and V_z, are calculated using Eq. (2) as

$$\begin{pmatrix} FRF_x \\ FRF_z \end{pmatrix} = \begin{pmatrix} cos\alpha_1 & cos\gamma_1 \\ cos\alpha_2 & cos\gamma_2 \end{pmatrix}^{-1} \begin{pmatrix} FRF_1 \\ FRF_2 \end{pmatrix} \tag{6}$$

3. Sensitivity of angles for accurate velocity measurement and noise reduction

If the two signals V_1 and V_2 are described as

$$\begin{aligned} V_1(t) &= Asin(wt) + N_1 \\ V_2(t) &= Bsin(wt) + N_2 \end{aligned} \tag{7}$$

where A and B are the amplitudes of V_1 and V_2, and N_1 and N_2 are the noise levels of V_1 and V_2. V_x and V_z can be obtained using Eqs. (4) and (5), as shown in Eqs. (8) and (9), respectively.

$$V_x + N_x = \frac{(Bcos\gamma_1 - Acos\gamma_2)sin(wt) + N_2 cos\gamma_1 - N_1 cos\gamma_2}{sin\gamma_1 cos\gamma_2 + cos\gamma_1 sin\gamma_2} \tag{8}$$

$$V_z + N_z = \frac{(Bsin\gamma_1 + Asin\gamma_2)sin(wt) + N_2 cos\gamma_1 + N_1 sin\gamma_2}{sin\gamma_1 cos\gamma_2 + cos\gamma_1 sin\gamma_2} \tag{9}$$

Herein, N_x and N_z are the noise levels of V_x and V_z respectively.

Fig. 3(a) shows the relation between the amplitude of V_x with respect to γ_1 and γ_2 for the in-plane vibration component when we consider $A = B = 1$ with no noise ($N_1 = N_2 = 0$). It is clear that V_x is very sensitive to γ_1 and γ_2 except in the case when the sum $\gamma_1 + \gamma_2$ is small and $\gamma_1 = \gamma_2$. Fig. 3(b) shows the relation between the amplitude of V_z with respect to γ_1 and γ_2 for out-of-plane vibrations. It is clear that V_z is very sensitive to γ_1 and γ_2 unless $\gamma_1 + \gamma_2$ is small. Therefore, it is recommended to choose angle values that satisfy the above conditions for reducing the sensitivity to γ_1 and γ_2 for accurate V_x and V_z estimation. The condition whereby $\gamma_1 = \gamma_2 = 45^\circ$ is a good example.

In addition to the possibility of inaccurate velocity measurements due to an erroneous selection of γ_1 and γ_2, the noise contained in the vibration signal can also be amplified thereby due to an erroneous selection of γ_1 and γ_2. For the consideration of only the effect of the angle variation to noise, we set $A = B = 0$. Eqs. (8) and (9) can then be rewritten in accordance to Eqs. (10) and (11), respectively.

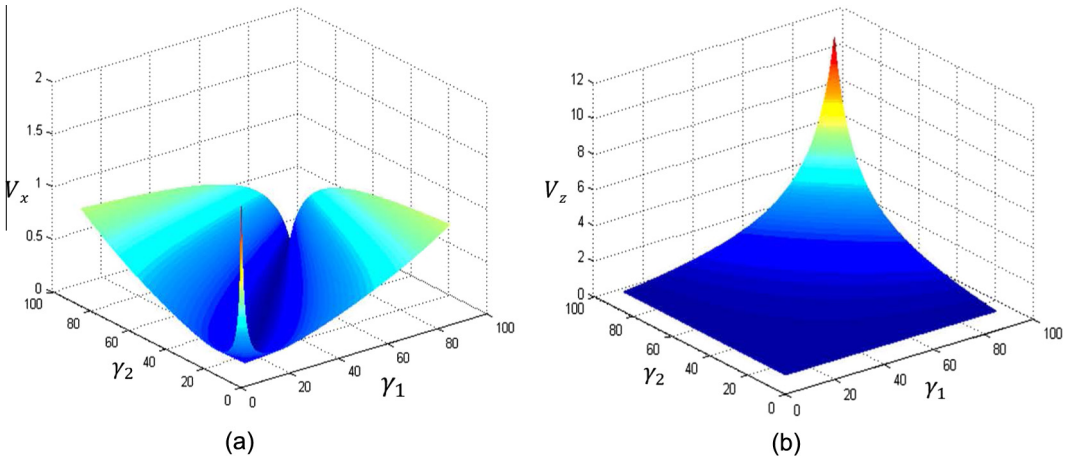

Fig. 3. (a) V_x versus γ_1 and γ_2, and (b) V_z versus γ_1 and γ_2.

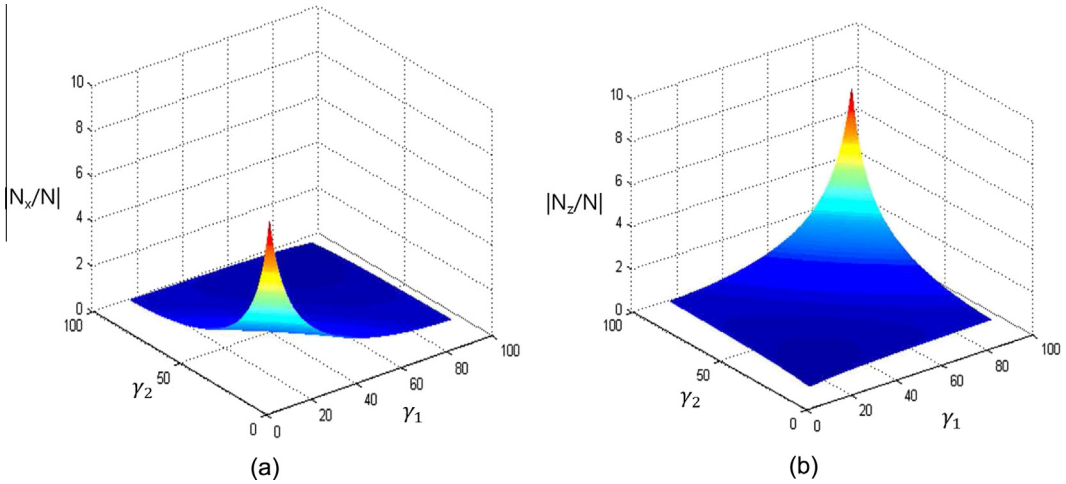

Fig. 4. (a) In-plane noise ratio $|N_x/N|$ versus γ_1 and γ_2, and (b) out-of-plane noise ratio $|N_z/N|$ versus γ_1 and γ_2.

$$N_x = \frac{N_2 cos\gamma_1 - N_1 cos\gamma_2}{sin\gamma_1 cos\gamma_2 + cos\gamma_1 sin\gamma_2} \quad (10)$$

$$N_z = \frac{N_2 sin\gamma_1 + N_1 cos\gamma_2}{sin\gamma_1 cos\gamma_2 + cos\gamma_1 sin\gamma_2} \quad (11)$$

Because only one set of LSV is used, the noise variations for V_1 and V_2 are considered to be the same, which indicates that $N_1 = N_2 = N$. The absolute values of noise ratios can be calculated as

$$\frac{|N_x|}{|N|} = \frac{\sqrt{cos^2\gamma_1 + cos^2\gamma_2}}{sin\gamma_1 cos\gamma_2 + cos\gamma_1 sin\gamma_2} \quad (12)$$

$$\frac{|N_z|}{|N|} = \frac{\sqrt{sin^2\gamma_1 + sin^2\gamma_2}}{sin\gamma_1 cos\gamma_2 + cos\gamma_1 sin\gamma_2} \quad (13)$$

As indicated by Eq. (12), the in-plane noise ratio N_x/N is minimized when the values of γ_1 and γ_2 are high. However, Eq. (13) indicates

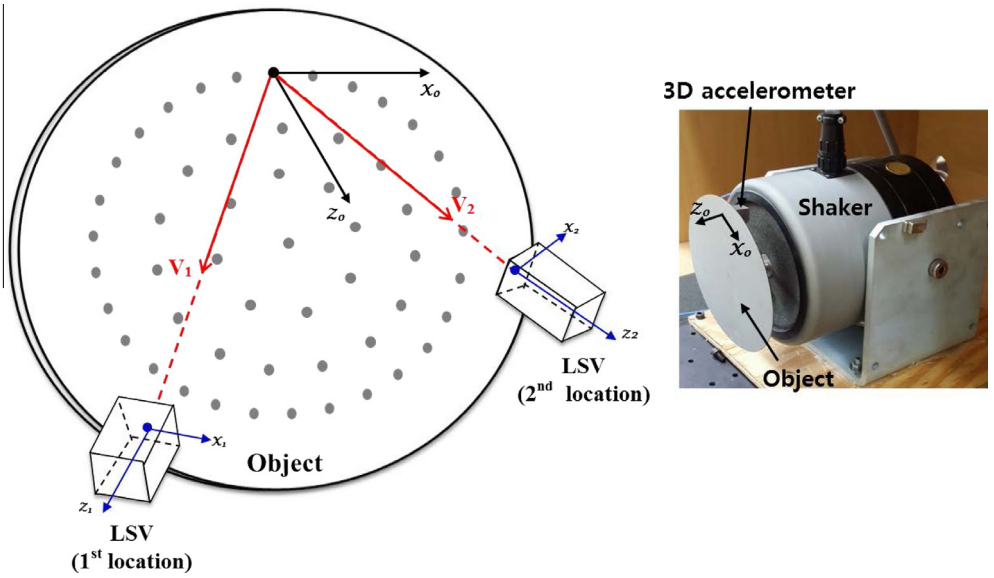

Fig. 5. Experimental set-up for 2D vibration measurements.

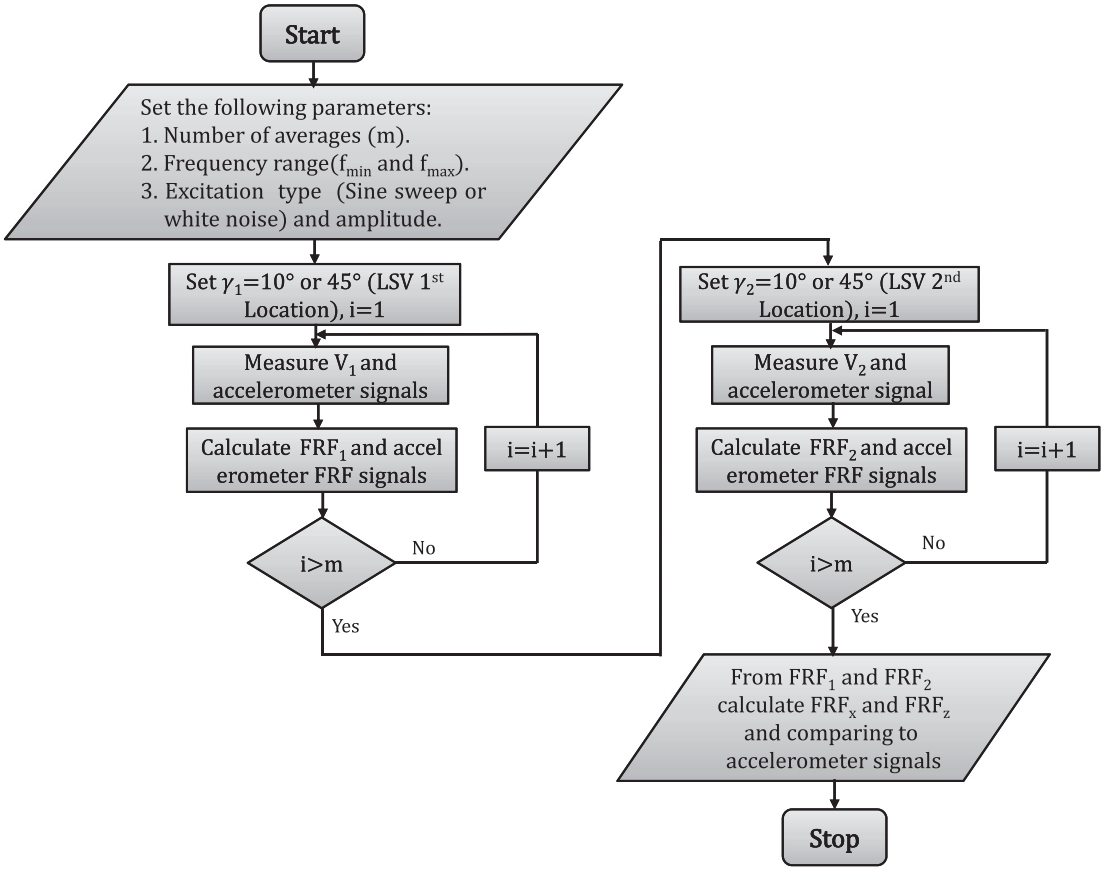

Fig. 6. Acquisition procedures for 2D vibration measurements.

that the out-of-plane noise ratio N_z/N is minimized when γ_1 and γ_2 are small. Fig. 4(a) and (b) shows how $|N_x/N|$ and $|N_z/N|$ vary with γ_1 and γ_2. From Fig. 4(a) and (b), γ_1 and γ_2 must be chosen to be close to 45° (i.e., γ_1=γ_2=45°) in order to elicit small noise ratios for both V_x and V_z.

According to accuracy and noise analyses, we can conclude that γ_1 and γ_2 must be chosen to be close to 45° for accurate and less noisy vibration measurements. If this result is extended to 3D vibration measurements, the angles with respect to the z_o-axis are called γ_k, where k = 1, 2, and 3, must be selected to be close to 45° for accuracy and noise suppression in 3D vibration measurements.

4. Experiment

4.1. 2D vibration measurement

Fig. 5 shows the experimental set-up for 2D vibration measurements. A shaker is used to excite the central point of the circular object having a radius of 75 mm in the z_o-axis direction. A sinusoidal sweeping signal is used as an excitation signal. All vibration measurements are performed using the LSV manufactured by EM4SYS Co., Ltd. [10]. All angles are adjusted by using an adjustable table to move the LSV to the desired direction with the desired

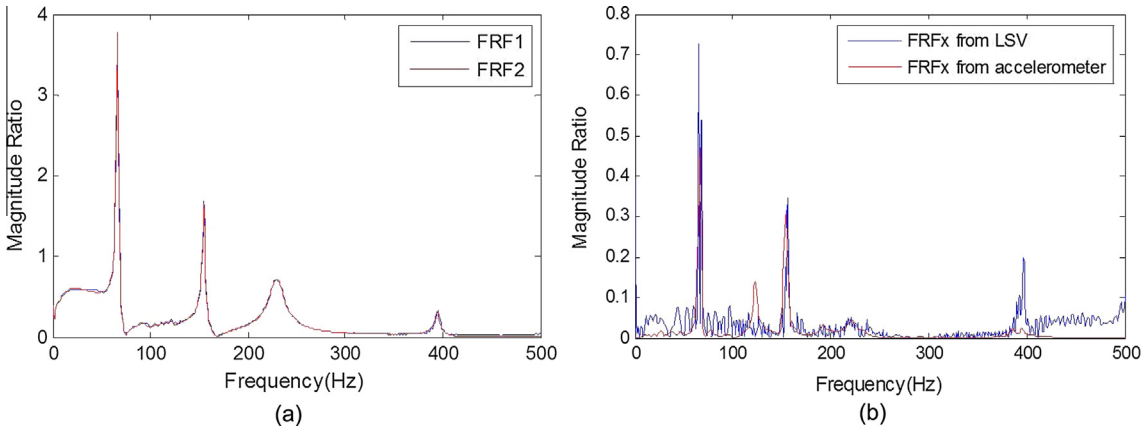

Fig. 7. (a) FRF_1 and FRF_2 calculated from the measured vibrations V_1 and V_2 at the angles of $\gamma_1 = \gamma_2 = 10°$, and (b) FRF_x obtained from the LSV and compared to that measured using a 3D accelerometer.

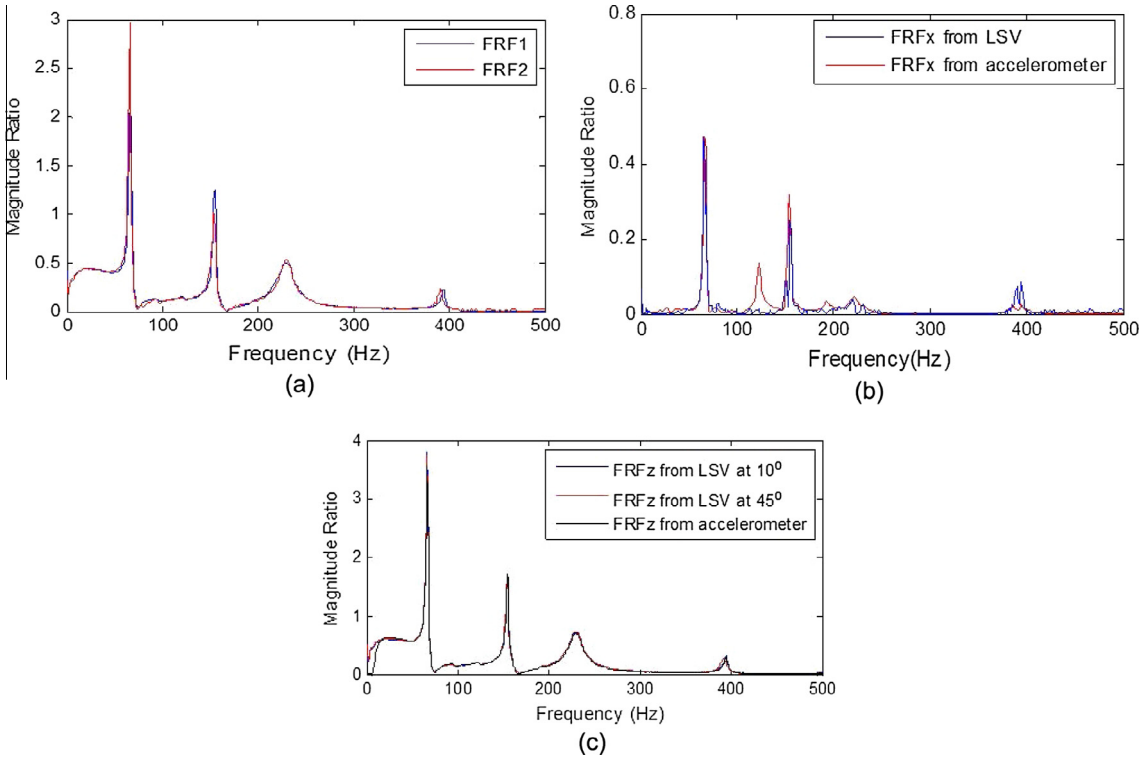

Fig. 8. (a) FRF_1 and FRF_2 calculated from the measured vibrations V_1 and V_2 at the angles of $\gamma_1 = \gamma_2 = 45°$, (b) FRF_x obtained from the LSV and compared to that measured using a 3D accelerometer and (c) FRF_z obtained from the LSV at $\gamma_1 = \gamma_2 = 10°$ and 45° and compared to that measured using a 3D accelerometer.

angle. The acquisition procedures for 2D vibration measurements are shown in Fig. 6.

Fig. 7(a) shows the frequency response functions (FRF_1 and FRF_2) calculated from the measured vibrations V_1 and V_2 at angles of $\gamma_1 = \gamma_2 = 10^\circ$. FRF_1 and FRF_2 are calculated with minimal noise in the results, as shown in Fig. 7(a). Fig. 7(b) shows the variation of FRF_x obtained from the LSV, calculated using Eq. (6), and compared to that measured using a 3D accelerometer. The 120 Hz resonance appeared in the elicited FRF_x result obtained using the 3D accelerometer is attributed to the noise power. However, the FRF_x, shown in Fig. 7(b) has a larger noise component compared to that measured using an accelerometer. In addition, the magnitude ratio is amplified significantly at resonant frequencies of 66 Hz, 386 Hz, and 394 Hz. The amplitude ratios of the signal at 386 Hz and 395 Hz measured by accelerometer are not accurately measured due to the mode coupling of the two resonant frequencies which affects the damping ratio at each natural frequency.

Table 1
Average values of normalized cross-correlations between LSV results and that obtained from accelerometer.

Angles	Normalized cross-correlations for FRF_x
$\gamma_1 = \gamma_2 = 10^\circ$	0.6588
$\gamma_1 = \gamma_2 = 45^\circ$	0.9748

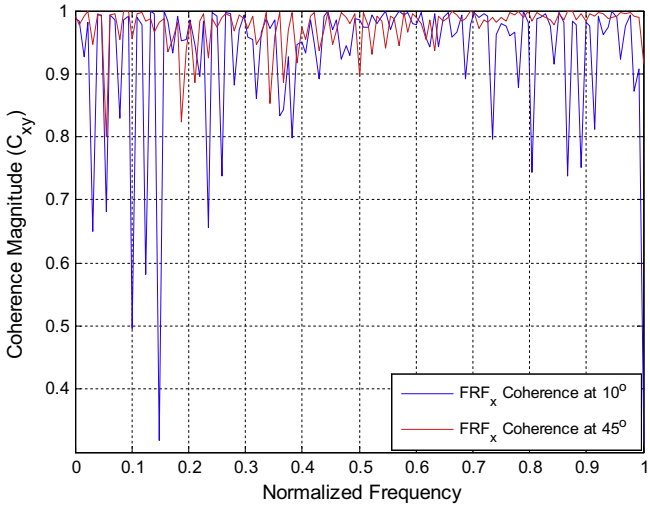

Fig. 9. Magnitude-squared coherence (C_{xy}) for FRF_x results between the LSV and accelerometer FRF results.

Fig. 8(a) shows the FRF_1 and FRF_2 calculated from the measured vibrations V_1 and V_2 at the angles of $\gamma_1 = \gamma_2 = 45^\circ$. FRF_1 and FRF_2 have little noise in the result, as shown in Fig. 8(a). Fig. 8(b) shows the FRF_x from LSV calculated using Eq. (6) and compared to the corresponding measurement using a 3D accelerometer. It can be easily observed that the FRF_x from the LSV is almost the same as that obtained by the accelerometer. In addition, it is more accurate and has a very small noise component compared to that obtained at the angles of $\gamma_1 = \gamma_2 = 10^\circ$ shown in Fig. 7(b). Fig. 8(c) shows the FRF_z from LSV at $\gamma_1 = \gamma_2 = 10^\circ$ and 45° calculated using Eq. (6) and compared to the corresponding measurement using accelerometer. It can be easily observed that the FRF_z obtained from LSV at both angles shows no significant variation comparing to that measured from the accelerometer.

From the FRF_x results obtained at both $\gamma_1 = \gamma_2 = 10^\circ$ and 45° as shown in Figs. 7(b) and 8(b) respectively. The normalized cross-correlation and magnitude-squared coherence (C_{xy}) are used as an indications for the accuracy and noise levels of the LSV results with respect to the accelerometer results. These indications are respectively defined by Eqs. (14) and (15).

$$Normalized - cross - correlation = \frac{1}{n}\frac{\sum_{i=1}^{N} x_i y_i}{\sqrt{\sum_{i=1}^{N} x_i^2 y_i^2}} \tag{14}$$

$$C_{xy}(f) = \frac{|P_{xy}(f)|^2}{P_{xx}(f)P_{yy}(f)} \tag{15}$$

where x is the FRF result of the LSV, y is the FRF result of accelerometer signal, N is the number of samples in the specified frequency

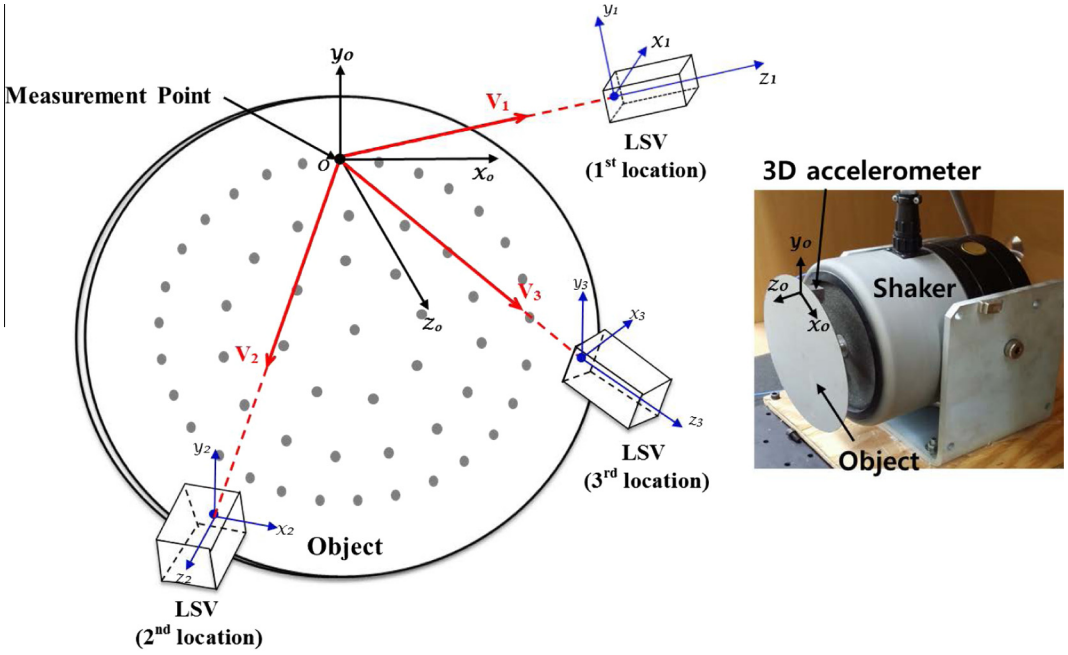

Fig. 10. Experimental set-up for 3D vibration measurements.

range and n is the number of measurements done to be averaged. $P_{xx}(f)$ and $P_{yy}(f)$ are the power spectral densities of x and y *FRF* signals. $P_{xy}(f)$ is the cross spectral density of x and y *FRF* signals.

The average of three measurements for normalized cross-correlation values between LSV results and that obtained from accelerometer are indicated in Table 1. Also, the coherence (C_{xy})

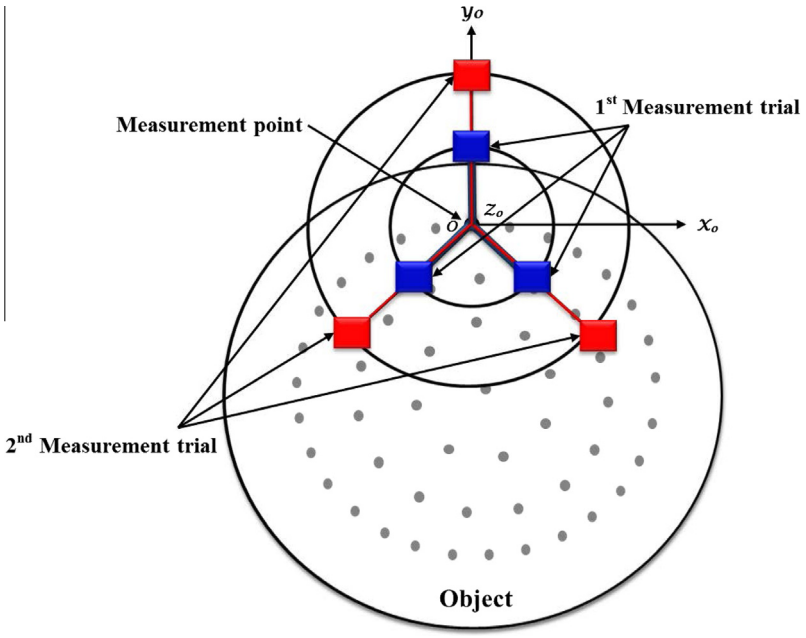

Fig. 11. Experimental setup for the two measurement trials at a 2D view.

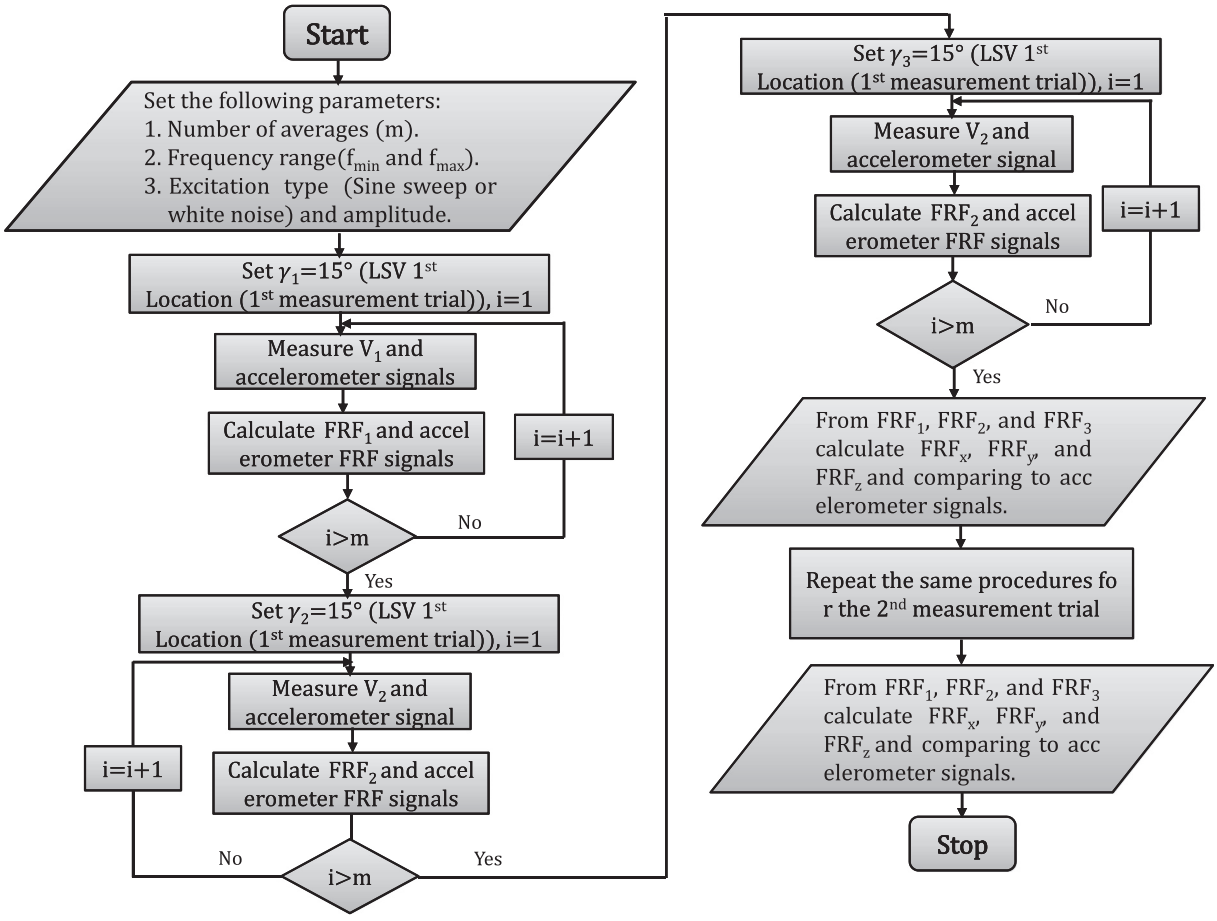

Fig. 12. Experimental acquisition procedures for obtaining FRF_x, FRF_y and FRF_z for each measurement trial.

between the x and y FRF signals is calculated as shown in Fig. 9. From results obtained in Table 1 and Fig. 9, it is noted that the LSV result for FRF_x at $\gamma_1 = \gamma_2 = 45^\circ$ is more accurate and less noisy comparing to that obtained at $\gamma_1 = \gamma_2 = 10^\circ$.

It is very interesting to note that even though we have good FRF_1 and FRF_2 signals, we can have inaccuracy and noise in the calculated results, depending on the angles γ_1 and γ_2. From these results, we can conclude that the more appropriate angles for 2D vibration measurements are $\gamma_1 = \gamma_2 = 45^\circ$. This is because an accurate FRF_x signal is obtained with less noise due to the less sensitivity to the errors and larger signal-to-noise ratio (SNR) resulting from lower noise amplification factor.

4.2. 3D vibration measurement

Based on 2D vibration measurements, it can be seen that the most appropriate angles with respect to the z_o-axis for measuring all the vibration components should be close to 45°, and for accurate and less noisy calculation of in-plane and out-of-plane vibration components. This is extended to 3D vibration measurements, which yields a similar conclusion, in that, γ_1, γ_2, and γ_3, must be chosen to be close to 45°.

Experimental set-up for 3D vibration measurements of an arbitrary point on a circular plate is shown in Fig. 10. The experimental set-up for the two measurement trials at 2D views is shown in Fig. 11. The first measurement trial is chosen to have small γ_1, γ_2, and γ_3 angles while the second measurement trial is chosen to have the suggested angles of 45° for γ_1, γ_2, and γ_3. The experimental acquisition procedures for obtaining FRF_x, FRF_y and FRF_z for each measurement trial are shown in Fig. 12.

Fig. 14(a) shows the FRF_1, FRF_2, and FRF_3, respectively calculated from the measured vibrations V_1, V_2, and V_3, at the angles of $\gamma_1 = \gamma_2 = \gamma_3 = 45^\circ$ for the 2nd measurement trial, as indicated in Table 2. FRF_1, FRF_2, and FRF_3, contain little noise in the result, as shown in Fig. 14(a). Fig. 14(b) shows FRF_x from the LSV calculated using Eq. (2) and compared to that measured using a 3D accelerometer. It is well observed that the FRF_x obtained from the LSV is almost the same as that obtained using the accelerometer. In addition, FRF_x is less noisy and more accurate compared to the results obtained at the angles of $\gamma_1 = \gamma_2 = \gamma_3 = 15^\circ$ shown in Fig. 13(b). Fig. 14(c) shows the FRF_y obtained from the LSV calculated using Eq. (2), and compared to that measured using a 3D accelerometer. It is observed that the FRF_y is much less noisy compared to that obtained at the angles of $\gamma_1 = \gamma_2 = \gamma_3 = 15^\circ$, shown in Fig. 13(c). Even though all the resonant frequencies are correctly identified in the LSV result, the magnitude ratio of the FRF_y obtained from the LSV is somewhat different from that obtained using the accelerometer. This is due to errors in the angle estimation and noise variation bounds.

Table 2
Estimated angles between the laser beam and local coordinates for the two measurement trials.

Angles	Estimated angles (1st measurement trial)	Estimated angles (2nd measurement trial)
α_1	90°	90°
β_1	75°	45°
γ_1	15°	45°
α_2	105°	135°
β_2	105°	135°
γ_2	15°	45°
α_3	75°	45°
β_3	105°	135°
γ_3	15°	45°

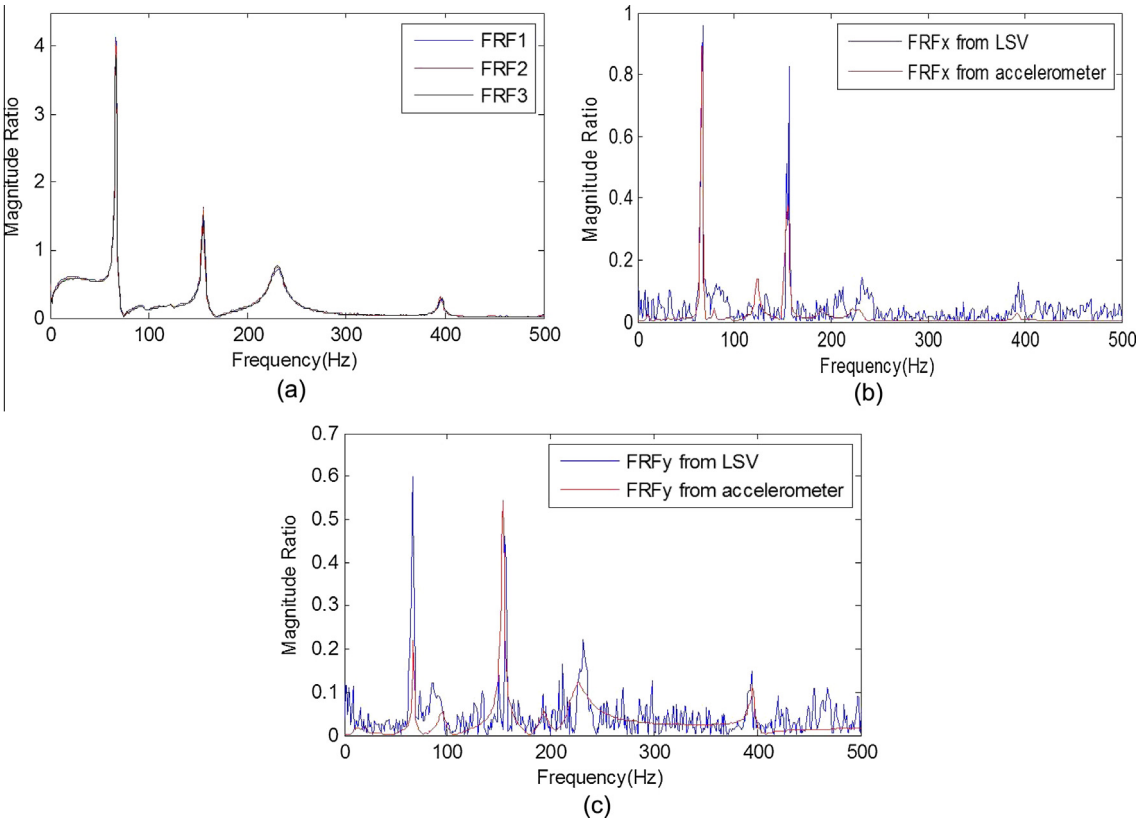

Fig. 13. (a) FRF_1, FRF_2, and FRF_3 calculated at the angles of $\gamma_1 = \gamma_2 = \gamma_3 = 15^\circ$ (1st measurement trial), (b) FRF_x from LSV and compared to that measured using a 3D accelerometer, and (c) FRF_y obtained from the LSV and compared to that measured using a 3D accelerometer.

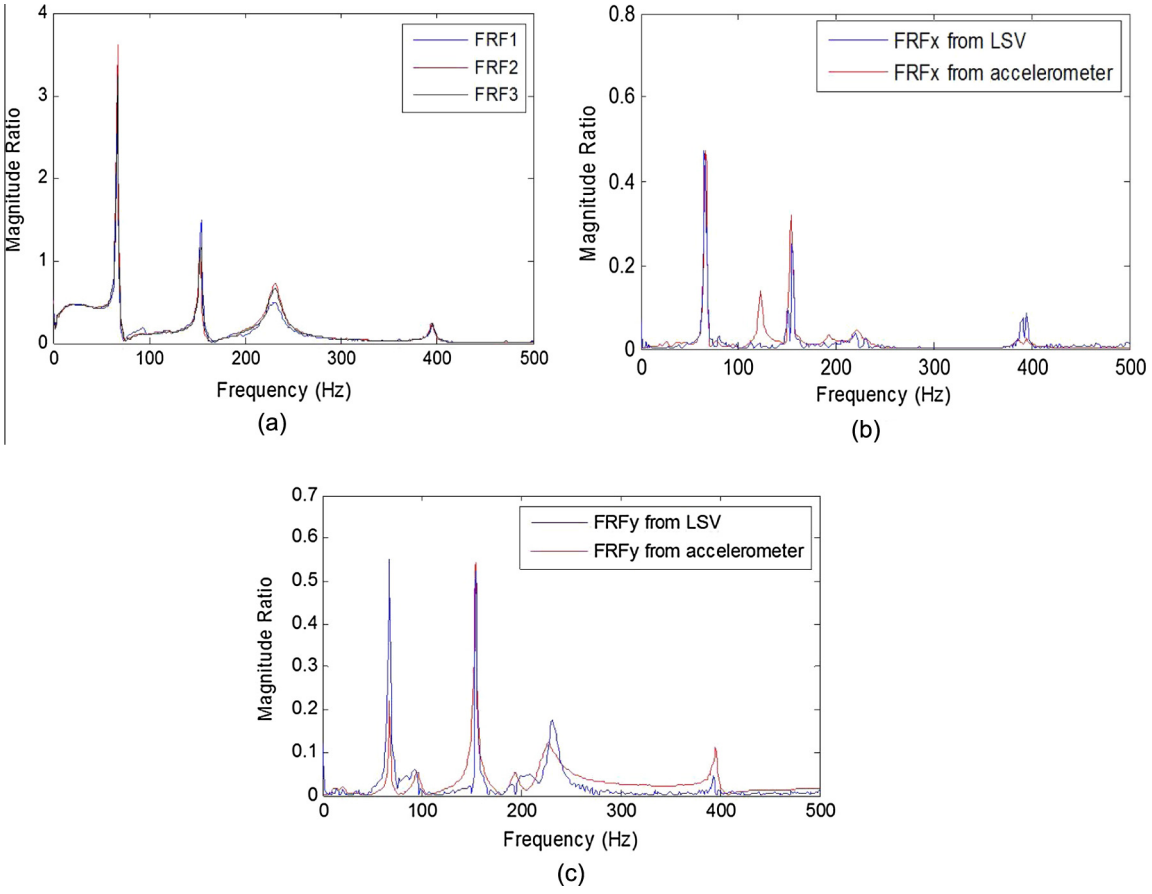

Fig. 14. (a) FRF_1, FRF_2, and FRF_3 calculated at the angles of $\gamma_1 = \gamma_2 = \gamma_3 = 45^\circ$ (2nd measurement trial), (b) FRF_x from LSV and compared to that measured using a 3D accelerometer, and (c) FRF_y obtained from the LSV and compared to that measured using a 3D accelerometer.

Table 3
Average values of normalized cross-correlations between LSV results and that obtained from accelerometer.

Angles	Normalized cross-correlations for FRF_x	Normalized cross-correlations for FRF_y
1st $\gamma_1 = \gamma_2 = \gamma_3 = 15^\circ$	0.6695	0.6787
2nd $\gamma_1 = \gamma_2 = \gamma_3 = 45^\circ$	0.9748	0.7746

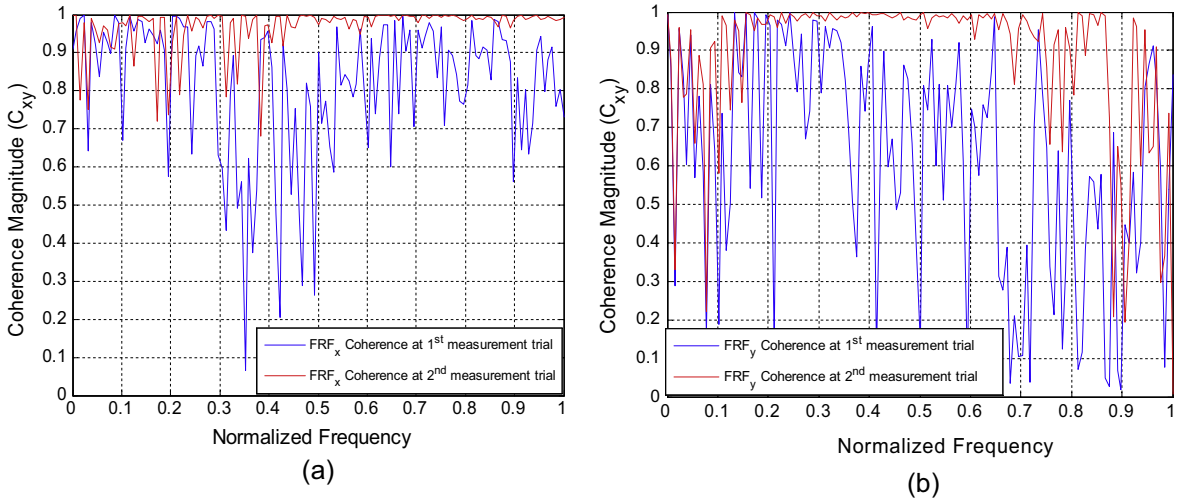

Fig. 15. Magnitude-squared coherence (C_{xy}) between LSV and accelerometer FRF results (a) for FRF_x, and (b) for FRF_y.

From the FRF_x results obtained at the two measurement trials as shown in Figs. 13(b) and 14(b) respectively, and also from the FRF_y results shown in Figs. 13(c) and 14(c) obtained at $\gamma_1 = \gamma_2 = \gamma_3 = 15^\circ$ and 45° respectively.The average values of normalized cross-correlations between LSV results and that obtained from accelerometer calculated using Eq. (14) are indicated in Table 3. Furthermore, the magnitude-squared coherence (C_{xy}) for both FRF_x and FRF_y at the two measurement trials are respectively calculated using Eq. (15). Fig. 15(a) and (b) shows the FRF_x and FRF_y coherence calculated between the LSV and accelerometer FRF results for both measurement trials. It is clear that the 2nd measurement trial (chosen angles) gives higher coherence values than that of the 1st measurement trial. From Table 3 and Fig. 15, it is clear that the LSV results for the 2nd measurement trial (chosen angles) are more accurate and less noisy comparing to that obtained for the 1st measurement trial. The FRF_z calculated for both measurement trials for both LSV and accelerometer shows no significant variations between each other as indicated in Fig. 8 (c) so the results are not introduced here.

It is very interesting to note that even though we have good FRF_1, FRF_2, and FRF_3 signals, we can have inaccuracies and noise in the calculated results depending on the angles γ_1, γ_2, and γ_3. From the 3D vibration results, we can conclude that the more appropriate angle for 3D vibration measurements is 45° because accurate FRF_x and FRF_y values are obtained in this case with much less noise.

5. Conclusions

Using the principle that vibration analysis in the frequency domain is independent of the vibration signal measured in time domain, 3D vibration measurements were performed using a single LSV by moving it to three arbitrarily different locations. The in-plane and out-of-plane vibration components are calculated using V_1, V_2, and V_3, measured at three different locations, and the angles between each LSV location and the local axis coordinates. The accuracy of the in-plane and out-of-plane vibration components can be degraded depending of the measurement angles. In addition to accuracy, the noise contained in the LSV is amplified depending on the measurement angles. Hence, it is necessary to introduce an analysis methodology for the angles so that the accuracy of the vibration measurement can be increased, and the noise minimized. The analysis on the angles is implemented theoretically for 2D vibration measurements first, and then the 3D vibration measurement methodology is addressed. Based on the theoretical 2D angle analysis, it can be concluded that the angles with respect to the z_0-axis, called γ_1 and γ_2 must be selected to be close to 45° for accurate and less noisy vibration measurements. The same conclusion can be extended to 3D vibration measurements so that the angles γ_1, γ_2, and γ_3 must be chosen to be close to 45°. Experiments are done for both 2D and 3D vibration measurements at small and suggested measurement angles, and the results are compared to those measured using a 3D accelerometer. It can be concluded that an erroneous selection of γ_1, γ_2, and γ_3 can elicit inaccurate and noisy vibration measurements. Based on the experiments, γ_1, γ_2, and γ_3, must be chosen to be close to 45° for more accurate and less noisy vibrations.

Acknowledgements

This work was supported by the National Research Foundation of Korea through the Korean Government under Grant 2011-0017876, and the New and Reliable Energy (20123030020010) of the Korea Institute of Energy Technology Evaluation and Planning (KETEP) Grant funded by the Korea government Ministry of Trade, Industry and Energy.

References

[1] J. La, J. Choi, S. Wang, K. Kim, K. Park, Continuous scanning laser Doppler vibrometer for mode shape analysis, Opt. Eng. 42 (3) (2003) 730–737.
[2] W.K. George, J.L. Lumley, The laser-Doppler velocimeter and its application to the measurement of turbulence, Fluid Mech. 60 (1973) 321–362.
[3] Sriram, S. Hanagud, J.I. Craig, Mode shape measurement using a scanning laser Doppler vibrometer, Int. J. Anal. Exp. Modal Anal. 7 (3) (1992) 169–178.
[4] P. Castellini, M. Martarelli, E.P. Tomasini, Laser Doppler vibrometry: development of advanced solutions answering to technology's needs, Mech. Syst. Signal Process. 20 (2006) 1265–1285.
[5] K. Bendel, M. Fischer, M. Schussler, Vibrational analysis of power tools using a novel three dimensional scanning vibrometer, in: Proceeding 6th International Conference Vibration Measurement Laser Technique, 2004, pp. 177–184.
[6] T. Miyashita, H. Ishii, K. Kubota, Y. Fujino, N. Miyamoto, Advanced measurement system using laser Doppler vibrometers for bridges, in: Proceeding of Conference and Exhibition on Structural Dynamics, 2007.
[7] M. Schssler, M. Mitrofanova, U. Retze, Measurement of 2D dynamic stress distributions with a 3D-scanning laser Doppler vibrometer, Top. Modal Anal. 3 (2011) 141–151.
[8] M. Fritzsche, J. Schell, W. Ochs, M.N. Neumann, R. Lammering, 3D scanning laser Doppler vibrometery for structural health monitoring using ultrasonic surface waves, in: 15th International Conference on Experimental Mechanics, 2012.
[9] D. Kim, H. Song, H. Khalil, J. Lee, S. Wang, K. Park, 3-D Vibration measurement using a single laser scanning vibrometer by moving to three different locations, IEEE Trans. Instrum. Meas. 63 (8) (2014) 2028–2033.
[10] EM4SYS Laser Scanning Vibrometer VIXCEL Series Manual, 2013. <http://www.em4sys.com/product/2013LSV/index.html#/0>.